

Deep-space Optical Terminals (DOT)

H. Hemmati, W. H. Farr, A. Biswas, K. M. Birnbaum,
W. T. Roberts, K. Quirk, and S. Townes

Jet Propulsion Laboratory, California Institute of Technology

ABSTRACT

A conceptual design study titled Deep-space Optical Terminals was recently completed for an optical communication technology demonstration from Mars in the 2018 time frame. We report on engineering trades for the entire system, and for individual subsystems including the flight terminal, the ground receiver and the ground transmitter. A point design is described to meet the requirement for greater than 0.25 Gb/s downlink from the nearest distance to Mars of 0.42 AU with a maximum mass and power allocation of 40 kg and 110 W. Furthermore, the concept design addresses link closure at the farthest Mars range of 2.7 AU. Maximum uplink data-rate of 0.3 Mb/s and ranging with 30 cm precision are also addressed.

1. INTRODUCTION

Optical communications has been identified as an emerging technology for providing a high-rate data-return service for NASA missions from lunar distances to throughout the solar system and beyond [1]. Deep space mission conditions cannot be fully emulated with near-Earth spacecraft carrying lasercom systems; therefore, for full mission acceptance precursor demonstrations are deemed necessary. Key among these conditions are large point-ahead angles, round-trip light times, and the simultaneous low Sun-Probe-Earth (SPE) and Sun-Earth-Probe (SEP) angles that result in low signal-to-noise ratios for both the optical transmit and receive stations. Moreover, the huge interplanetary distances call for aggressively efficient (high bits/photon) modulation and coding strategies that result in requiring high peak-to-average power laser transmitters that are unproven in the space environment.

In 2003 NASA initiated the Mars Laser Communication Demonstration (MLCD) Project, which progressed through a successful preliminary design review but was aborted in mid-2005 due to cancellation of the host spacecraft [2,3]. In 2009, the Deep-space Optical Terminals (DOT) study was initiated with a key objective of demonstrating *an order of magnitude higher downlink data rate* with a flight terminal mass and power comparable to current NASA deep-space telecom systems. The primary motivation for augmenting NASA's telecommunication data-rates is to enhance the science data volume returned from higher resolution instruments, and prepare for future human deep-space exploration missions [4]. The Deep-space Optical Terminals (DOT) concept design study targets the first deep-space opportunity that becomes available for demonstrating bidirectional lasercom between Earth and deep space.

The DOT system is composed of four major subsystems, as shown in Figure 1:

1. The DOT Mission Operations Center (MOC) controls DOT operations and performs data analysis and archiving;
2. The Ground Laser Transmitter (GLT) sends an uplink beam to the spacecraft [5]. The uplinked beam is used as a pointing reference (i.e., beacon) at the spacecraft, as well as, for transmitting uplink data.
3. The Flight Laser Transceiver (FLT) is the DOT subsystem mounted on the spacecraft that receives the uplink beacon and transmits a downlink beam [6]; and
4. The Ground Laser Receiver (GLR) receives the downlink light and recovers the communication data.

2. SYSTEMS ENGINEERING

The DOT study was conducted without a specific host spacecraft. Instead, reasonable assumptions for a deep-space spacecraft were made in developing the concept design. The spacecraft platform disturbance is a key driver influencing the design of the challenging laser beam pointing control assembly. Disturbance power spectral densities from past spacecraft such as Olympus, Cassini, Spitzer, and OICETS were studied as elaborated in Ref. 7. An enveloping disturbance spectrum was derived as a guideline for the FLT design. This resulted in an angular power spectral density (PSD) of $1\text{E-}7 \text{ rad}^2/\text{Hz}$ at and below 0.1 Hz;

1E-15 rad²/Hz at 1 kHz with a 20 dB/decade slope beyond 0.1 Hz, as shown in Figure 2. The RMS angular disturbance resulting from this assumed PSD is 140 μrad.

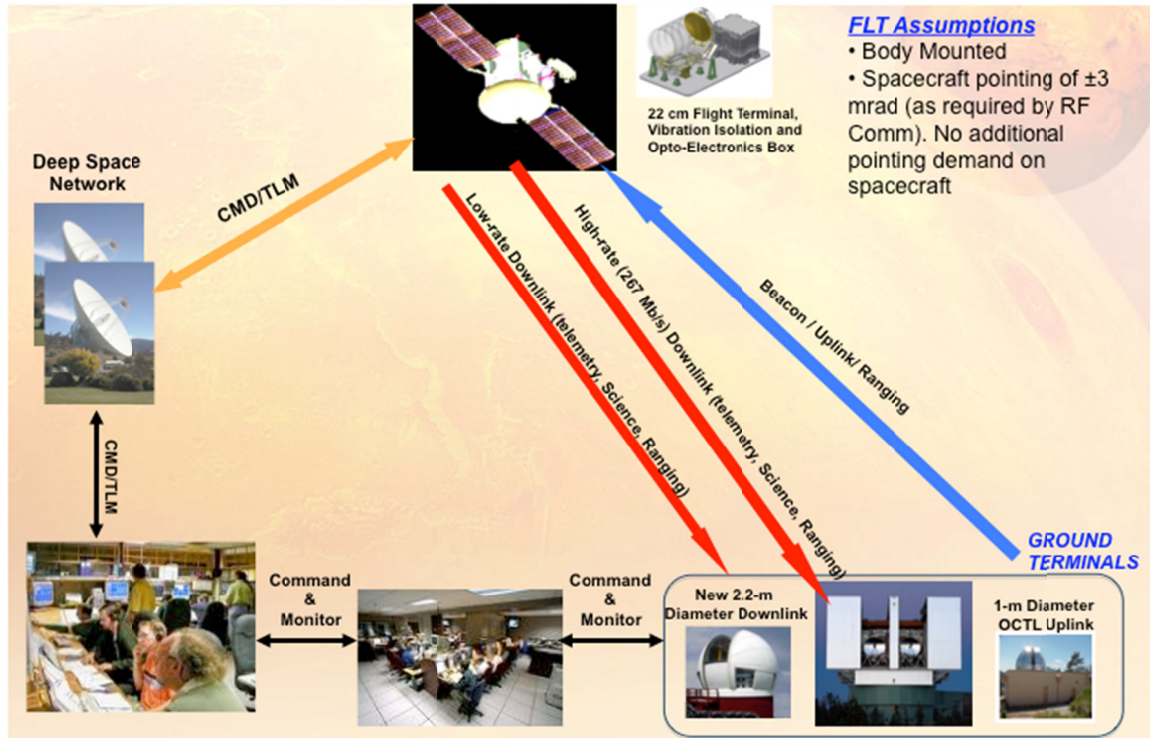


Figure 1. DOT system architecture. The GLR accepts the downlink photons from the FLT and sends the decoded data to the DOT MOC.

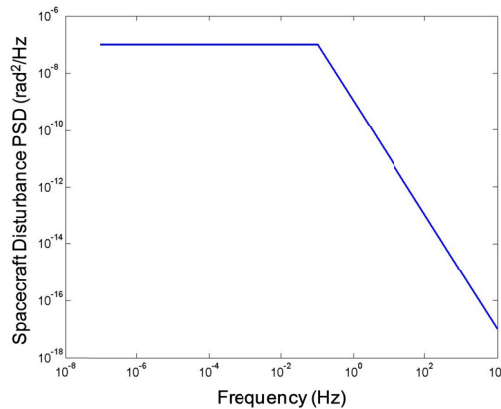


Figure 2: The angular disturbance power spectral density (PSD) derived as an envelope from the measured PSD’s of previously flown spacecraft, such as, Olympus, Cassini, Spitzer, and OICETS.

The objective of the signaling trade was to achieve maximum power efficiency (bits/photon) while preserving DOT system implementation and operations simplicity. The major signaling selection decisions were: the detection method; range of slot-widths; modulation; error-correction-code; and synchronization markers.

Downlink Signaling Trades: The primary functions of the downlink signaling are to support the range of targeted downlink data-rates (e.g. the maximum data-rate >0.25 Gb/s at 0.42 AU) with high power efficiency and to aid in downlink temporal acquisition and supp. Direct and coherent detection were considered. Direct detection in conjunction with photon-counting (DD-PC) data reception was selected since it was determined that for the DOT operating regime this technique is more power efficient than coherent detection. Pulse position modulation (PPM) was selected over alternatives due to its near-optimum

power efficiency at the targeted operating regime, and low implementation complexity [8]. The PPM orders were determined by data-rate requirements and peak power limitations of the laser transmitter, which limits the maximum supportable PPM order. For DOT the maximum PPM order was 128. To maintain a low implementation risk for the flight avionics a minimum slot width of 0.5 ns was chosen. Candidate error correction codes (ECC) focused on modern, iteratively decoded codes, which provide high power efficiency. The serially concatenated PPM (SCPPM) encoding was baselined for the optical downlink. SCPPM in conjunction with photon-counting direct-detection receiver has been demonstrated to achieve communications performance within 1 dB of theoretical limits [9]. Table 1 summarizes the DOT downlink and uplink signaling trades.

Table 1. Summary of DOT signaling trades.

		Detec-tion	Min/max slot-width	Modula-tion	Sync Markers	ECC	Data Rates
Downlink		DD-PC	0.5 ns/ 256 ns	PPM 16, 32, 64, 128	25% guard-time	R=1/3,1/2, 2/3 SCPPM	13 kb/s, 57 kb/s,...,267 Mb/s (26 points in ~1.5 dB steps)
Uplink	Sync	DD-PC	164 μ s	Square Wave	None	None	None
	Command	DD-PC	82 μ s	PPM 2	100% guard-time	R=191/25 5 Reed-Solomon	9.0 b/s
	Data	DD-PC	128 ns/ 16 μ s	PPM 16	25% guard-time	R=191/25 5 Reed-Solomon	2.3,...,292 kb/s (7 points in ~2.2 dB steps)

Uplink Signaling Trades: The uplink signaling functions are: providing a reference beacon; aiding synchronization; supporting a low-rate command capability for near-real-time link control; transmitting high-rate uplink data at near Mars ranges; and supporting ranging. DD-PC is again selected from a consideration of photon-efficiency and the relatively high bandwidth that photon-counting detectors can afford for communications and ranging. Mass and power savings are key benefits of selecting DD-PC implemented as a detector array with a field of view (FOV) that covers the range of point-ahead angles. This enables implementation of beam pointing, synchronization, commanding, high-rate data communications link and ranging with a single sensor (detector array and read-out circuitry). Nested within the synchronization pattern is a binary (M=2) PPM signal for the low rate commanding, with a laser pulse-width (slot-width) of 82 μ s and an equivalent guard-time to aid synchronization. Nested in this pulse the high-data rate signaling corresponding to a PPM modulation with an order M=16 and a slot-width of 128 ns. A Reed-Solomon (255,191) code was selected for the uplink due to its low complexity and ability to provide a low undetected error rate on the uplink channel.

Laser Wavelength Trades. Besides link efficiency, transmit-receive-wavelength isolation at the FLT was an important wavelength selection consideration. The relative difficulty of obtaining high power 1550 nm lasers for uplink coupled with the availability of kWatt power level 1-micron lasers favors the choice of 1550 nm for downlink and 1030 nm for uplink to enhance transmit-receive wavelength isolation. For uplink wavelength selection, the availability and performance characteristics of uplink photon counting detectors were a major driver. Selection of the uplink laser beam divergence was driven by the requirement to ensure that the designed beam divergence can deliver the requisite mean irradiance to the DOT flight terminal aperture. A peak-to-peak beam pointing error of 16 μ rad, and an air mass corresponding to a 70° zenith angle were assumed. The selection was a beam divergence between 30-40 μ rad with 40 μ rad favored for strong to moderate atmospheric turbulence represented by $r_0 = 3$ to 10 cm.

The downlink budget is summarized in Figure 3 for a 22-cm flight terminal aperture and 4-W transmit laser power. Note the optical data-rate performance versus distance to Mars does not follow inverse square distance dependence, as does the Ka-band because with increasing distance the SEP angles get smaller and the additive background noise penalty on the link throughput increases.

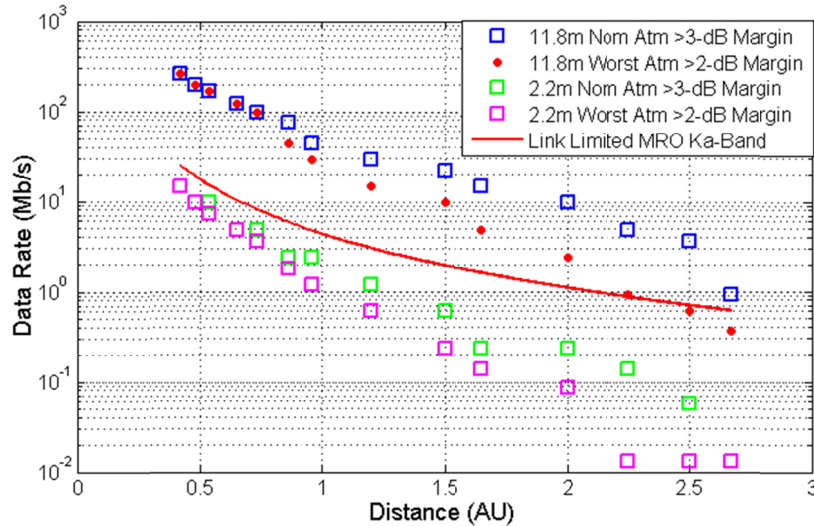


Figure 3. Downlink performance summary for nominal and worst conditions using the 11.8 m LBT telescope (blue squares and red dots) and a 2.2 m telescope. The link-limited Ka-band performance (solid line) is included for reference.

Uplink budgets were analyzed at the nearest and farthest Mars range. PPM-16 with Reed-Solomon is used for the inner modulation and error-correction code. The spot size is assumed to cover a 2 x 2 pixel sub-array of the uplink photon-counting array detector with an instantaneous field-of-view (IFOV) of 8- μ rad per pixel. With 1.2 kW of laser power transmitted from the ground, a data-rate of 292 kb/s with a 3-dB margin is achieved.

2. FLT – FLIGHT LASER TRANSCEIVER

The intent of FLT’s technology validation in space is to: (a) retire the major perceived risks of operational deep space optical telecommunications; and (b) demonstrate a flight terminal concept that is easily scalable from data rates of hundreds of Mb/s to a few Gb/s at spacecraft ranges out to at least 5 AU (Jupiter). Beyond this range a beaconless acquisition and tracking architecture will likely be required. The FLT architecture is comprised of the four major assemblies (Fig. 4). The “optical head” includes sub-assemblies (e.g. transmit/receive telescope, aft optics, acquisition/tracking/data sensors, and a point-ahead mirror) that are isolated from the spacecraft by a low-frequency vibration-isolation platform (LVP). The LVP attenuates angular disturbances of the host spacecraft to facilitate meeting precision pointing requirements. Those sub-assemblies (e.g. laser transmitter, modems, controllers, processors and power converters) that do not need to be vibration-isolated are located in the “optoelectronics” assembly. Fine copper and fiberoptic cables (arranged in an umbilical cord) carry power, electrical and optical signals between the two assemblies. Care must be taken to avoid mechanically short-circuiting the LVP’s isolation function.

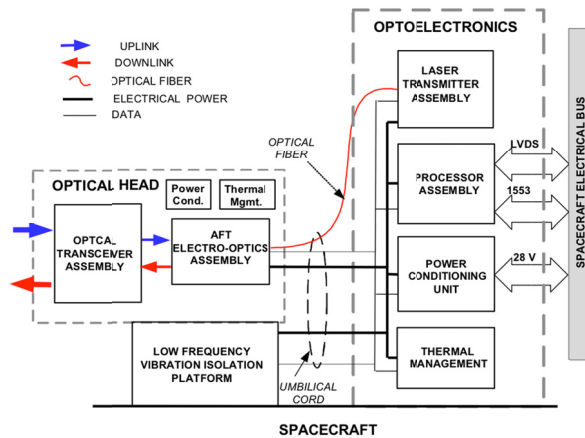


Figure 4. FLT major assemblies reference architecture.

Pointing, Acquisition, and Tracking implementation is a major FLT concept design driver, especially due to the combination of dim beacon tracking and the requirement for low mass and power terminal. The pointing loss requirement calls for derived sub-micro-radian ($1-\sigma$) transmit beam pointing in the presence of greater than 0.1 mrad of angular disturbance from the spacecraft primarily due to imperfect attitude control, and reaction wheel vibrations. As a result, the LVP sub-assembly (supplanted by fine steering on the transmit beam) must reduce spacecraft-induced angular disturbances by over two orders of magnitude. The LVP is designed to mitigate the majority of host-platform-induced angular disturbances, using both passive isolators and active control by the processor sub-assembly.

Accommodation of the large point-ahead angular range of ± 400 micro-rad at an arbitrary roll angle is another major design driver. Since closed-loop confirmation of transmit beam pointing across the multi-minute light propagation times at deep space ranges is impractical, a common transmit/receive optical aperture provides the highest pointing stability. In this case, the requirement on the focal-plane-sensor's field-of-view is a minimum of 400 micro-rad to simultaneously detect both the transmit and the receive (beacon/data) beams. The pointing error control table has contributions from (shot) noise on the received beacon signal in beacon tracking sensor, and from control bandwidth limitations in platform and beam steering actuators. Typical control bandwidth limits are ~ 100 Hz for a beam steering mirror, ~ 4 Hz for local pointing control of the optical head, and ~ 0.1 Hz for control of the spacecraft.

Laser Transmitter. The laser transmitter modulated the incoming encoded signal onto the transmit beam. For modulation, the link analysis suggests PPM symbols with 16 to 128 slots per symbol, plus an additional 25% for the inter-symbol guard time for PPM16 (for synchronization) [10]. This sets a requirement on laser transmitter peak-to-average power ratios ranging from 20:1 to 160:1, with laser pulse-widths ranging from 0.5-ns to 8-ns. Repeating the PPM symbols forms logical slot-widths greater than 8-ns. Either a master-oscillator power-amplifier a fiber or bulk crystal, or waveguide slab is the most suitable configurations for the laser, considering the difficulties in acquiring proper modulation format from a high power oscillator.

Erbium-doped fiber-amplifier (EDFA) based sources at 1550 nm are readily available but at much lower peak-to-average power ratios than required to support the SCPPM encoding. Large-mode-area co-doped Er-Yb fiber amplifiers optically pumped with 976-nm diodes, followed by multiple gain stages provide sufficient average and peak power performance to meet the FLT requirement. Fiber nonlinearities such as stimulated Brillouin scattering or stimulated Raman scattering limit the peak power of fiber-based amplifiers. Initial measurements on existing PPM fiber-amplifier-based transmitters suggest an 8 ns pulse-width is feasible using an expanded-mode area fiber. Figure 5 schematically illustrates the baselined concept in which a DFB diode laser is used as the oscillator.

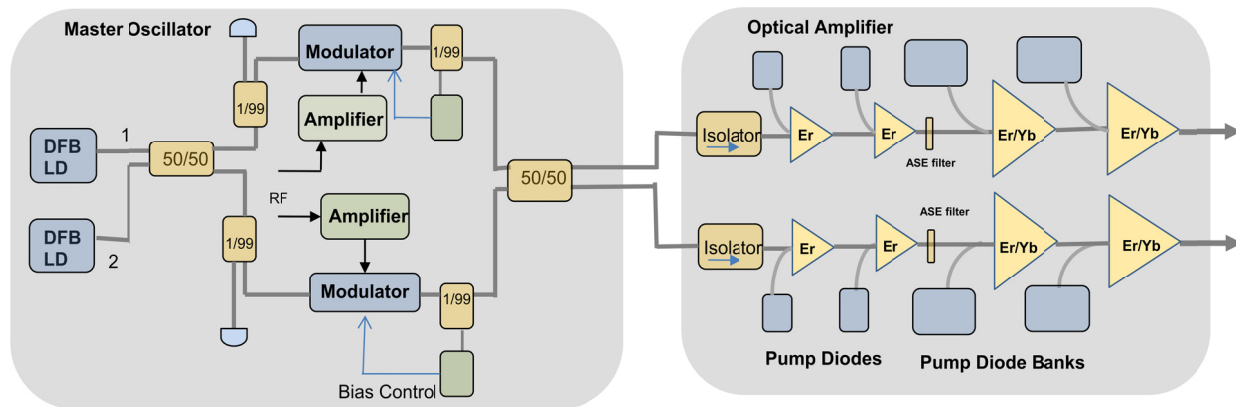


Fig. 5. Laser transmitter conceptual design.

Uplink Sensor. This sensor detects the uplink data, tracks uplink beacon, and simultaneously tracks the downlink beam to verify the point-ahead angle. For the uplink wavelength of 1030-nm, silicon, germanium, InGaAs, and InGaAsP are also viable candidate detector materials though silicon contributes the lowest noise. The downlink wavelength (1550 nm) may also be tracked on a silicon detector via two-photon absorption [11]. Moreover, use of the non-1550 nm sensitive detector then becomes advantageous due to the inherent transmit-receive isolation afforded by the absorber physics. To meet FLT requirements, technology development and a future down select between Resonant Cavity Enhanced (RCE) Silicon Geiger-Mode or Negative Avalanche Feedback (NAF) InGaAsP technologies, both operating in the photon-counting mode, is

planned. The backup option of a deep-depletion Si CCD with a separate channel for uplink data is possible, albeit with mass/power penalties resulting in a reduced uplink data rate (due to the higher detector noise of a linear mode detector).

Aperture Configuration and Size. Different optical antenna configurations and their relative impacts on transmit beam quality and near-sun-pointing performance and survival (with and without the use of a filter at the entrance aperture of the telescope), were evaluated. Mass and manufacturability were estimated as a function of aperture size to trade against laser transmitter power required to achieve required downlink signal level and beacon detection efficiency. A 22-cm diameter off-axis Gregorian telescope provided the highest combination of overall performance with the lowest mass for the FLT [Fig. 6]. The Gregorian field stop prevents secondary mirror thermal warping in near-Sun operations and strongly limits scattered light. A silicon carbide primary and structure was selected for lowest mass and superior thermal distortion characteristics.

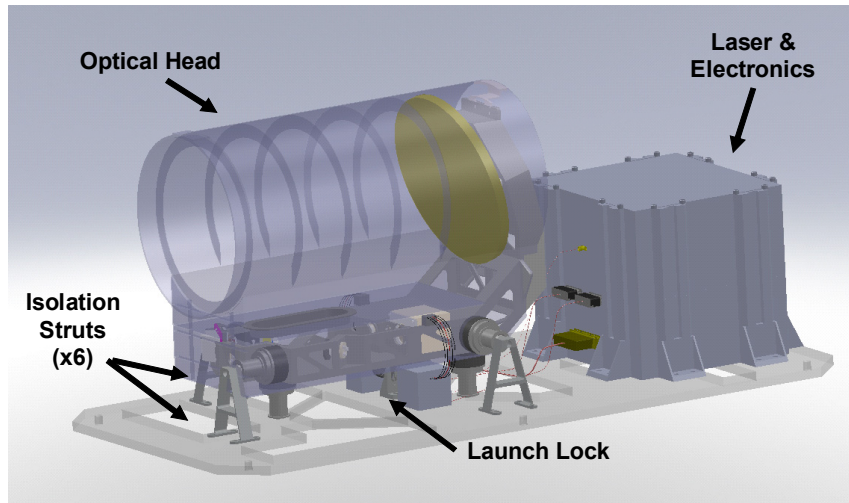


Fig. 6. Schematic of the FLT

3. GLR – GROUND LASER RECEIVER

There are four major factors that drive the design of the GLR subsystem:

1. Large net gain requirement: this demands the use of a large collecting area, as well as highly efficient optics and detectors for receiving the faint signal from deep space;
2. Daytime and low SEP angle operations requirement: this is unusual for telescopes, which are typically designed to operate only at night (or in the case of solar telescopes, only while pointing directly at the Sun);
3. Low rate of signal photons: the link operates in the photon-starved regime, which necessitates the use of efficient modulation and error-correcting codes to maximize the bits per photon [9]. This ultimately impacts the electronics used to receive and decode the downlink signal: and
4. Low ratio of signal photons to background photons: the detected rate of background photons may exceed the rate of signal photons by as much as 18 dB during low SEP operations. This increases the difficulty of performing spatial and temporal acquisition of the signal. It also makes it necessary to precisely filter the incoming light to keep the background rate as low as possible while minimizing the loss of the signal photons.

Taking into account optical losses, the required GLR telescope aperture gain of 142 dB for the high data-rate link translates to 110 m² aperture (11.8-m in diameter). Similarly, an aperture gain of 124 dB for the low data-rate link translates to a ground aperture of 3.8 m² area (2.2 m in diameter). Table 2 compares the requirements on a ground telescope for lasercom with a typical astronomical telescope. These relaxed requirements on the lasercom telescope result in significantly lower cost for the lasercom telescope compared to an astronomical telescope of the same diameter.

Table 2. Comparison of requirements on astronomical quality and lasercom telescopes

Telescope for:	Astronomy	Lasercom
Maximum image spot size (μrad)*	~2 to 5	~20
Telescope filed-of-view (μrad)	200 to much larger	~50
Near sun pointing requirement	No	Yes
Source spectrum	Broadband	Monochromatic
Point/extended source	Both	Point

* Depending on the atmospheric seeing of the site

Employing extremely low-noise single-photon-sensitive detectors for data detection allows the use of a single aperture or an array of telescopes each equipped with a data detector [12]. With these considerations in mind, a number of point designs for low-cost telescopes were created. The figure of merit is taken to be the cost of a telescope assembly divided by its effective area of light collection. Note that the telescope assembly cost includes not only the cost of the telescope optics, but also the cost of mounts, gimbal, dome, site preparation work, etc. (excluding the opto-electronic receiver cost). The relative figures of merit of the point designs are shown in Figure 3.

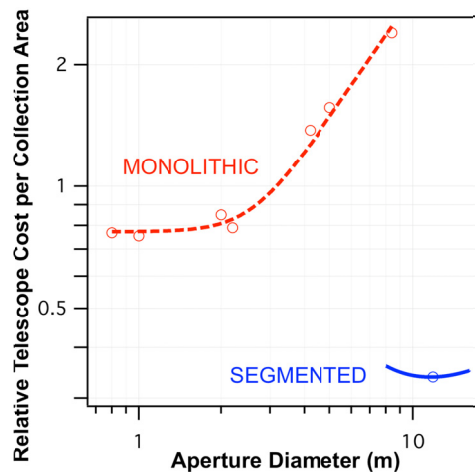


Figure 3. The relative cost of building a telescope assembly per collecting area (in arbitrary units) vs. diameter of the collecting aperture. Circles indicate point designs, while smooth curves are based on parametric scaling.

Both monolithic primary mirror designs with diameters between 0.8 m and 8.2 m, and segmented primary mirrors were investigated. The cost curve for monolithic mirrors shows a knee with a nearly constant cost per area for apertures below 2.2 m. Above 2.2m diameter, the cost per area increases nearly proportional to diameter [13,14]. Based on this analysis, for a monolithic primary design the lowest cost build approach meeting the requirements is an array of 2.2-m terminals. For a large segmented primary design, we find that a 12-m telescope is near the minimum of the cost curve ($\pm 50\%$ of area without major change in cost/area).

Based on the DOT project goals, including minimizing cost and risk, as well as providing feed forward to future capabilities, the baseline approach chosen was that of renting the Large Binocular Telescope for high data-rate links and building a new 2.2-m telescope with near-Sun pointing capability for low data-rate links. For the initial operational capability, after successful demonstrations of the DOT terminals, we recommend pursuing the ground receiver approach based on a large segmented primary mirror telescope.

The aft optics assembly relays the signal light from the telescope assembly to the detector assembly while rejecting the background light. The primary trade here is the choice of technology for spectral filtering. The volume Bragg grating (VBG) was selected for the baseline design because of its narrow bandwidth, large acceptance angle and high efficiency [15,16]. The architecture of the aft optics assembly is shown in Figure 7.

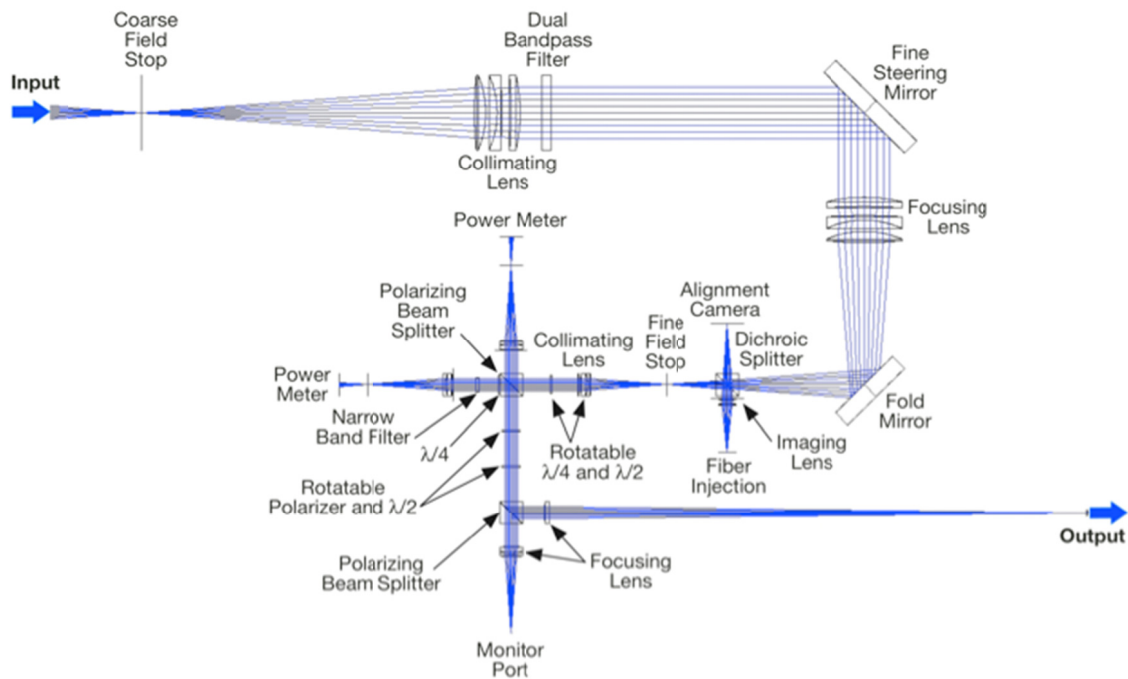


Figure 7. The architecture of the aft optics assembly. The path marked “Input” comes from the telescope assembly, and the path marked “Output” goes to the detector assembly.

The Detector Assembly’s driving requirements are: array format with minimum of three sets of pixels, detection efficiency >50%; dark count rate <0.33 MHz; timing jitter <120 ps; and etendue $>3.9 \times 10^{-8} \text{ m}^2\text{sr}$. Currently, the high required etendue can only be achieved by arraying many pixels. Also, given the high count-rates expected in the link, spreading the light over many pixels is required in order to avoid blocking losses due to the saturation of each pixel. The superconducting nanowire single-photon detectors (SNSPDs) offer the best combination of high timing resolution, high saturation rate, and high detection efficiency [17,18].

With today’s technology, arrays of several hundred elements have to be developed with sufficient collecting area, but the performance of each pixel (timing jitter, in particular) meets requirements. The intensified photodiode (IPD) meets nearly all requirements [19]. However, it suffers from relatively low detection efficiency of 30% at 1550 nm. Based on the state of the art, the baseline concept of the GLR is to develop large arrays of SNSPDs for the GLR detector assembly, while the IPD will be kept as a low-risk backup.

Electronics Assembly. This assembly processes the detector signal and determines the number of photons received in each temporal slot in each region, synchronizes to the downlink signal, estimates the rate of signal and background photons, and controls the acquisition and tracking of the downlink. The electronics assembly has to have the capability to process a range of incoming signal formats including variable data-rates, variable PPM orders, code rates, slot widths, symbol repetitions, and background photon rates. Enough flexibility is required to reconfigure to any operating point within 5 min. In addition to the 1.2 dB gap to capacity for the serially concatenated pulse-position modulation (SCPPM) code, 1.5 dB of implementation loss is allocated to the processing electronics [12].

A solution developed under a NASA technology program was baselined. This architecture, which is scalable to data-rates exceeding 1 Gb/s was validated in emulated links [20]. The six major subassemblies include: the programmable oscillator, receiver, channel combiner, and signal acquisition/tracking controller within the element electronics; and the channel combiner/de-interleaver and decoder in the station electronics.

4.0 GLT – GROUND LASER TRANSMITTER (GLT)

The key driving GLT requirements are summarized in Table 3.

Table 3. Uplink Transmit Beacon Requirements

Requirement	Comment
Uplink power	Power exiting system
Number of beams	For atmospheric fade reduction
Beam Divergence	Narrow beams to reduce required power
Pointing accuracy	Must meet this 99% of time
Near Sun Angle	Operate to within this angle of Solar Limb
Beam Separation	Beam edges must be at least this far apart

The GLT must blanket the region of space surrounding the FLT with a uniform irradiance sufficient to reliably be seen by the FLT's image sensor. Due to the extreme distance between the two terminals, meeting this requirement involves transmission of high levels of power (2.5 KW) in a narrow (40 μ rad), accurately pointed beam. To achieve this, the uplink stations must be able to blind-point the beam with an accuracy of 16 μ rad to limit the beam-pointing loss to an acceptable level. Multi-beam uplink is baselined to mitigate uplink atmosphere-induced fades by propagating at least 9 separate beams (or beam sets) each separated from all of the others by at least 10 cm.

Uplink telescope. A single telescope, distributed (arrayed) telescopes, and flat-mirror beam directors are all capable of meeting the requirements stated above. The existing 1-m diameter coudé path OCTL telescope is favored based on availability, cost and complexity. This telescope has already demonstrated the required pointing, though it is expected that it will improve beyond its current accuracy with the implementation of certain planned upgrades.

Uplink laser. The key laser requirements include: 1030 nm wavelength, 0.5 nm line-width and ± 0.1 nm wavelength tunability, 2.5 kW average and 370 kW of peak power with $M^2 < 1.2$ beam quality, pulse repetition rates in the 4 to 500 kHz range, 128 ns pulse-width, random polarization, and 20 dB pulse extinction ratio. There are two candidate beacon laser options: (1) a set of single spatial mode 1030 nm fiber amplifiers for which CW power of about 250 Watts has been demonstrated, and (2) the planar waveguide amplifiers, where a single laser or a number of lasers can satisfy the requirements. Depending on the chosen candidate laser system, some minor level development is expected to demonstrate the aggregate set of laser requirements.

5. CONCLUSION

A pair of flight and ground terminals were conceptually designed to meet the Level 1 requirements, enabling downlink transmission of over 0.25 Gb/s from the short distance to Mars while estimated flight terminal mass power are comparable to the state of practice of existing Mars spacecraft telecommunication systems. Currently, the highest risk items are the technology maturity of the flight isolation platform, the flight laser, and the flight and the ground single photon-sensitive data detectors. These specific technologies are now being addressed in a focused technology development program. Accomplishing the highest data-rates requires use of the Large Binocular Telescope with its effective aperture diameter of 11.8 m. Demonstrating operations at small Sun angles necessitates development of a dedicated telescope with minimum aperture diameter of 2.2 m.

Acknowledgements: The work described here was performed at the Jet Propulsion Laboratory (JPL), California Institute of Technology under contract with the National Aeronautics and Space administration (NASA).

REFERENCES

1. H. Hemmati, "Deep Space Optical Communications," Wiley Interscience, 2006.
2. D. M. Boroson, A. Biswas, B. L. Edwards, "MLCD: Overview of NASA's Mars laser Communications Demonstration System" Free-Space Optical Comm. Tech., XIV, Proc. SPIE, vol. 5338, pp. 16-28, 2004.
3. A. Biswas, D. M. Boroson and B. L. Edwards, "Mars laser Communications Demonstration: What it could have been," Free-Space Optical Comm. Tech, XVI, Proc. SPIE, V. 6105, pp. 610502-1 to 6105052-12, 2006.
4. Space Communications and Navigation (SCaN) Integrated Network Architecture Definition Documents (ADD), Volume 1: Executive Summary, Revision 1, 2010.
5. W. T. Roberts and M. W. Wright, "Deep-space Optical Terminals (DOT) Ground Laser Transmitter (GLT): Trades and Conceptual Point Design," to be published in The Interplanetary Network Progress Report, vol. 42-183, Jet Propulsion Laboratory, Pasadena, California, November 15, 2010.
6. W. H. Farr, M. W. Regehr, M. W. Wright, A. Sahasrabudhe, J. W. Gin, and D. H. Nguyen, "Overview and Trades for DOT Flight Laser Transceiver," to be published in *The Interplanetary Network Progress Report*, vol. 42-184, Jet Propulsion Laboratory, Pasadena, California, February 15, 2011.
7. W. Farr, M. Regehr, M. Wright, A. Sahasrabudhe, J. Gin, and D. Nguyen, "Overview and Trades for the DOT Flight Laser Transceiver," to be published in The Interplanetary Network Progress Report, vol. 42-184, Jet Propulsion Laboratory, Pasadena, California, February 15, 2011.
8. J. Hamkins, "Pulse position modulation," "Handbook of Computer Networks," H. Bidgoli, Ed. New York Wiley, Ch. 37, 2007.
9. B. Moision and J. Hamkins, "Coded modulation for the deep space optical channel: serially concatenated PPM," JPL's IPN Progress Report, vol. 42-161, 2005.
10. K. J. Quirk, J. W. Gin, and M. Srinivasan, "Optical PPM synchronization for photon counting receivers," Military Communications Conference, 2008. MILCOM 2008. IEEE, pp.1-7, 16-19 Nov. 2008.
11. G. G. Ortiz, W.H. Farr "Two-Photon Absorption Long Wavelengths Optical Beam Tracking," IPN Progress Report 42-173, 2008. http://ipnpr.jpl.nasa.gov/progress_report/42-161/161T.pdf
12. K. Quirk and J. Gin, "Optical PPM Combining Loss for Photon Counting Receivers," *IEEE Military Communications Conference*, pp. 1-4, October 2006. <http://dx.doi.org/10.1109/MILCOM.2006.30>, 1986.
13. J. R. Lesh and D. L. Robinson, "A Cost-Performance Model for Ground-Based Optical Communications Receiving Telescopes," *The Telecommunications and Data Acquisition Progress Report*, vol. 42-87, pp. 56-64, November 15, 1986, issue dated July-September 1986. http://ipnpr.jpl.nasa.gov/progress_report/42-87/87G.PDF
14. T. Schmidt-Kaler and P. Rucks, "Telescope Costs and Cost Reduction," *Proceedings of SPIE*, edited by A. L. Ardeberg, vol. 2871, pp. 635-640, 1997. <http://dx.doi.org/10.1117/12.269092>.
15. J. Lumeau, L. B. Glebov, and V. Smirnov, "Tunable Narrowband Filter Based on a Combination of Fabry-Perot Etalon and Volume Bragg Grating," *Optics Letters*, vol. 31, no. 16, pp. 2417-2419, 2006. <http://dx.doi.org/10.1364/OL.31.002417>
16. D. Caplan, P. Chapnik, J. Carney, M. Stevens, M. Willis, and M. Glynn, "Narrow-Band Low-Loss Multi-Mode Spectral Filtering for Free-Space Optical Receivers," *IEEE LEOS*, pp.163-165, 2008. <http://dx.doi.org/10.1109/LEOS.2008.4688539>
17. J. Stern and W. Farr, "Fabrication and Characterization of Superconducting NbN Nanowire Single Photon Detectors," *IEEE Trans. on Applied Supercond.*, vol. 17, pp. 306-309, June 2007. <http://dx.doi.org/10.1109/TASC.2007.898060>
18. X. Hi, et. al., "Fiber-Coupled Nanowire Photon Counter at 1550nm with 24% System Detection Efficiency," *Optics Letters*, V.34, 3607-3609, 2009.
19. R. La Rue, G. Davis, D. Pudvay, K. Costello, and V. Aebi, "Photon Counting 1060 nm Hybrid Photomultiplier with High Quantum Efficiency," *IEEE Electron Devices Lett.* Vol.20, pp. 1126-128, 1999.
20. K. Birnbaum, W. Farr, J. Ginn, B. Moision, K. Quirk, and M. Wright, "Demonstration of High-Efficiency Free-Space Optical Communications Link," *Proc. Pf SPIE*, vol. 7199, p. 71990A, 2009.